Biosensors and Bioelectronics 26 (2011) 4162–4168

Contents lists available at ScienceDirect

Biosensors and Bioelectronics

journal homepage: www.elsevier.com/locate/bios

Biosensor for direct cell detection, quantification and analysis

Sandra Cortès[a,b], Christian L. Villiers[a,b], Pascal Colpo[c], Rachel Couderc[a,b], Carine Brakha[a,b], François Rossi[c], Patrice N. Marche[a,b], Marie-Bernadette Villiers[a,b,*]

[a] INSERM, U823, Grenoble, F-38042, France
[b] Université J. Fourier, UMR-S823, F-38042, France
[c] European Commission Joint Research Centre, Ispra (VA), Italy

ARTICLE INFO

Article history:
Received 12 January 2011
Received in revised form 7 April 2011
Accepted 8 April 2011
Available online 15 April 2011

Key words:
Surface plasmon resonance imaging
Cell
Antibody
Polyethylene oxide
Biological samples
Receptor

ABSTRACT

Microarrays are promising tools for cell isolation and detection. However, they have yet to be widely applied in biology. This stems from a lack of demonstration of their sensitivity and compatibility with complex biological samples, and a lack of proof that their use does not induce aberrant cellular effects. Herein, we characterized and optimized a recently developed technology associating antibody microarrays with surface plasmon resonance imaging (SPRi). Using a murine macrophage cell line we demonstrate the binding specificity of our antibody-microarrays and the correlation between SPRi signals and both the number of bound cells, and the level of expression of cell surface markers. Confocal microscopy reveals that cell binding to the chip through antibody–antigen interactions underwent morphological changes reflecting the density of the relevant cell surface marker without affecting cell viability as shown by fluorescent microscopy. The detection threshold of the microarray–SPRi system is lowered 10-fold by applying a polyethylene oxide film to the gold surface of the chip. This increased sensitivity allows the detection of cells representing as little as 0.5% of a mixed population. The potential of this method is illustrated by two applications: characterization of ligand–cell receptor interactions, allowing determination of receptor specificity, and analysis of peripheral blood mononuclear cells, demonstrating the suitability of this tool for the analysis of complex biological samples.

1. Introduction

Antibody (Ab) based microarrays are used for both applied and basic biological research. Their applications are developed for the analysis of protein expression, protein–protein interactions or pathogen infection and to perform drug research or disease diagnosis (for review, see Wingren and Borrebaeck, 2006). Although significant advances have been made over the past decade, applications of microarrays remain limited by various fundamental problems such as low sensitivity or incompatibility with complex biological samples. Traditional cell detection methods for low cellular concentrations require either labeling or enrichment, which both suffer from low efficacy due to the loss of cells during processing. Moreover, these approaches must be adapted for the analysis of complex biological samples. Identification and isolation of rare cells (virus-infected or tumor cells) in clinical samples constitute major challenges for both biological and medical research. For example, several studies have demonstrated that virus-specific cytotoxic T lymphocytes play a key role in the control of viral infections (Dorries, 2001; Thimme et al., 2003; Walker et al., 2010). However, studies of T lymphocyte specificity are limited by the low proportion of specific cells present in samples (blood or biopsies). In order to better exploit such cellular samples, a detection method which is both discriminative and sensitive must be developed. We have already described a system allowing label-free and real-time cell detection and measurement, which is composed of an Ab microarray (specific for cell surface markers) and surface plasmon resonance imaging (SPRi) (Suraniti et al., 2007; Villiers et al., 2010). The use of this system in a wide range of applications requires the characterization of diverse parameters: thus, cell behaviour and viability will influence downstream *in silico* analyses of cellular response while sensitivity and compatibility with complex biological samples will condition the pertinence of the system for clinical investigations.

In this article, we first characterize the system by analyzing the influence of the cell surface marker targeted by the immobilized Ab on SPRi signal and on the behaviour of the cells once bound to the chip surface. We also demonstrate the harmlessness of the method on the cells. In order to decrease the detection threshold and enhance the sensitivity and specificity of the detection, we have modified the microarray surface with polyethylene oxide (PEO) deposition, which is known to have cell-repellent properties (Bretagnol et al., 2006). This modification improves the potential

* Corresponding author at: INSERM, U823, Institut Albert Bonniot, BP170, F-38042 GRENOBLE Cedex 9, France. Tel.: +33 4 76 54 94 33; fax: +33 4 76 54 94 14.
E-mail address: Marie-Bernadette.Villiers@ujf-grenoble.fr (M.-B. Villiers).

0956-5663/$ – see front matter © 2011 Elsevier B.V. All rights reserved.
doi:10.1016/j.bios.2011.04.016

of the system for the analysis of biological material and enlarges its applicability. As proofs of concept, we provide results from two applications, namely: the study of cell receptor specificity and the analysis of human peripheral blood mononuclear cell population.

2. Experimental

2.1. Cell lines

Cell lines were from the American Type Culture Collection (Rockville, MD, USA). The murine macrophage cell line J774 (ATCC TIB-67) and the human promyelocytic cell line HL60 (ATCC CCL240) were grown in Dulbecco's modified eagle medium and RPMI1640 (Gibco, France), respectively, supplemented as described in Supplementary data. All cultures were incubated at 37 °C in a humidified 5% CO_2 incubator.

Before injection of cells, Fc gamma receptors (FcgR) were blocked by pre-incubating the cells for 15 min in either 15% mouse or human serum, or 83 nM mouse Fc Block (BD Pharmingen, Le Pont-de-Claix, France). Then, cells were washed twice in phosphate saline buffer (PBS) and resuspended in PBS/bovine serum albumin (BSA) 0.5% at 1×10^6 cells mL^{-1}. Cell viability was assayed by ethidium bromide/acridine orange (EB/AO) staining (Parks et al., 1979).

2.2. Preparation of human peripheral blood mononuclear cells

Blood samples from healthy volunteers were obtained from the Etablissement Français du Sang (La Tronche, France). The study was in agreement with the recommendations of the local ethic committee. Peripheral blood mononuclear cells (PBMC) were isolated using standard Ficoll-Hypaque (Eurobio, France) centrifugation, washed twice in PBS and resuspended in PBS/FCS 1% at 1×10^6 cells mL^{-1}.

2.3. Antibodies

mAb against mouse or human cell surface markers were purchased from BD Pharmingen and from Clinisciences (Montrouge, France) (Supplementary Table 1).

2.4. Materials and reagents for SPR analyses

Glass prisms coated with a 50 nm gold layer were obtained from Genoptics-HORIBA Scientific (Chilly-Mazarin, France). PEO deposition (10 nm-thick) was realized as detailed in Supplementary data. Pyrrole–mAb conjugates were generated as described (Grosjean et al., 2005).

2.5. Antibody immobilization on gold

mAb were immobilized on the gold surface of the biochip by electrochemical copolymerization of pyrrole–mAb conjugates (2 μM) (Cherif et al., 2006). Each Ab was spotted in triplicate using an Omnigrid robotic arrayer (Genoptics-HORIBA Scientific); 81 spots (500 μm diameter) can be deposited on 1 cm surface of the biochip. The prism was rinsed with distilled water and saturated at room temperature (RT) for 30 min with 1 mg mL^{-1} poly(L-lysine)–graft–(polyethylene glycol) co-polymer (SurfaceSolutionS GmbH, Zurich, Switzerland) in PBS. The chip was then incubated for 10 min in PBS/tween-20 0.05% (Sigma–Aldrich, St. Quentin-Fallavier, France), saturated with PBS/BSA 2% (10 min), washed with distilled water and used immediately.

2.6. Antibody immobilization on PEO

mAb (2 μM) in PBS/glycerol (10%, w/v) were immobilized on PEO by adsorption. mAb were microspotted directly onto the PEO surface in triplicate. Once the drop dry (20 h RT), the chip was rinsed with distilled water and used immediately.

2.7. Biochip-based cell capture and SPRi detection

All reactions were carried out in PBS/BSA 0.5% (RT) in a 14 μL peek chamber, at a flow rate of 100 μL min^{-1}. After cell injection (500 μL, different concentrations), the chip was rinsed with PBS-BSA to remove unbound cells. For each experiment, all injections were carried out successively, without chip regeneration. Cell binding was monitored as detailed in Supplementary data, using SPR imager (SPRi-Lab, Genoptics-HORIBA Scientific) connected to a Waters 600E pump (Millipore, Lyon, France). Data were analyzed using SPRi1000 software.

2.8. Flow cytometry analyses

Cells (1×10^6 cells) were incubated with labeled Ab (Pernollet et al., 2002). Flow cytometry analyses were performed on a FACSAria (BD Bioscience) and data were treated using FCS Express V3 (De Novo Software, Thornhill, Canada). Dead cells were excluded from analyses by gating on propidium iodide negative cells.

2.9. Confocal microscopy

Cells (10^6 mL^{-1}) were deposited on a glass coverslip coated either with a gold film grafted with pyrrole–mAb conjugates (similar to the biochip) or with poly-L-lysine for 45 min before fixing with paraformaldehyde (Villiers et al., 2008). Then cells were incubated with 0.4 μM FITC-labeled cholera toxin fragment B (Sigma–Aldrich,) for 30 min and observed using a confocal microscope (Zeiss LSM 510 NLO) with 488 nm excitation wavelength and 0.5 μm depth of focus.

3. Results

3.1. Analysis by SPRi of cell binding to the Ab chip

The principle of the method is to immobilize on the chip surface Ab directed against cell membrane proteins in order to capture cells from an injected mixed sample. We have previously demonstrated that this system allows cell specific binding which can be detected by SPR imaging (Villiers et al., 2010). To further characterize the system, we have analyzed the influence of the grafted Ab on cell trapping. For this, different monoclonal Ab (mAb) were grafted on the gold surface: anti-CD86 and anti-CD11b (macrophage-specific Ab) and anti-CD8 and anti-CD90 (isotypic controls). Cells from the murine macrophage cell line J774 were mixed with HL60, a human promyelocytic cell line which does not express CD86, CD11b, CD8 and CD90 as controlled by flow cytometry. A mixed sample containing J774/HL60 (1/3, total cell number 200,000) was injected onto the chip. Cell binding on immobilized Ab modified the refractive index near the chip's surface, resulting in a change of reflectivity (ΔR). As shown Fig. 1a, the reflectivity on anti-CD86 and anti-CD11b spots increased upon cell injection reaching plateau after 35 min, whereas very low or no signal was observed on the negative controls (anti-CD8, anti-CD90 and polypyrrole alone). Furthermore, the modification of the SPR signal varied according to the grafted Ab, anti-CD86 leading to a higher signal than anti-CD11b.

The reflectivity increase was related to cell binding by analysis of the biochip's SPR image (Fig. 1b): bound cells were visualized as white dots present only on anti-CD86 and anti-CD11b spots. Because the SPR image provides a weak resolution and relatively deformed view of these cells, cellular binding was confirmed by direct observation by microscope of the prism after removal from

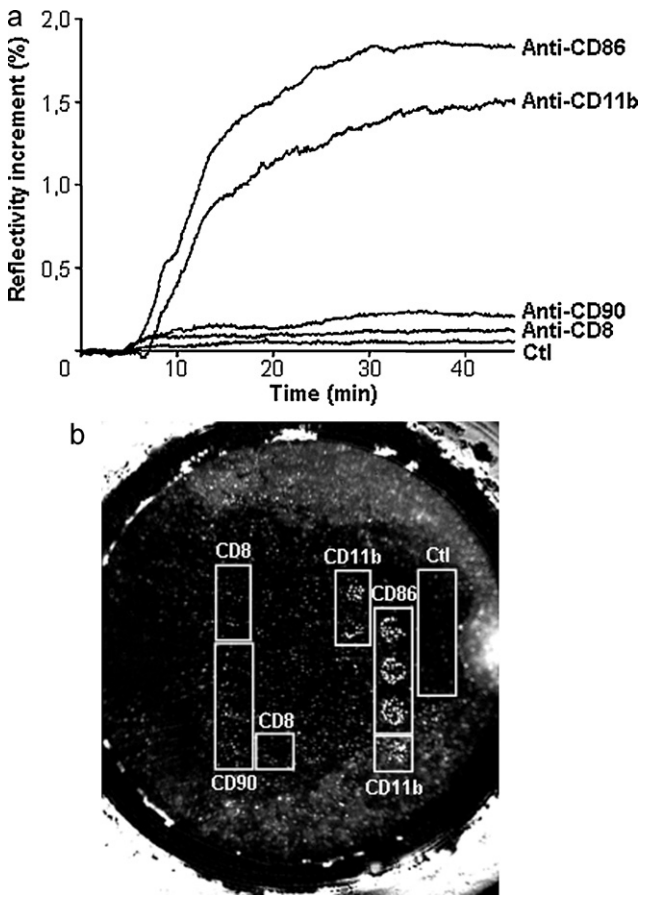

Fig. 1. Cell binding to an Ab chip. J774 (5×10^4), pre-incubated with 15% mouse serum to block FcgR, were injected ($t = 0$ min) onto a chip on which mAb (2 μM) were grafted. Cell binding was monitored by SPRi. (a) Sensorgrams following cell injection. (b) SPR differential image of the chip. Ctl = control (polypyrrole without mAb). This experiment is representative of four independent assays.

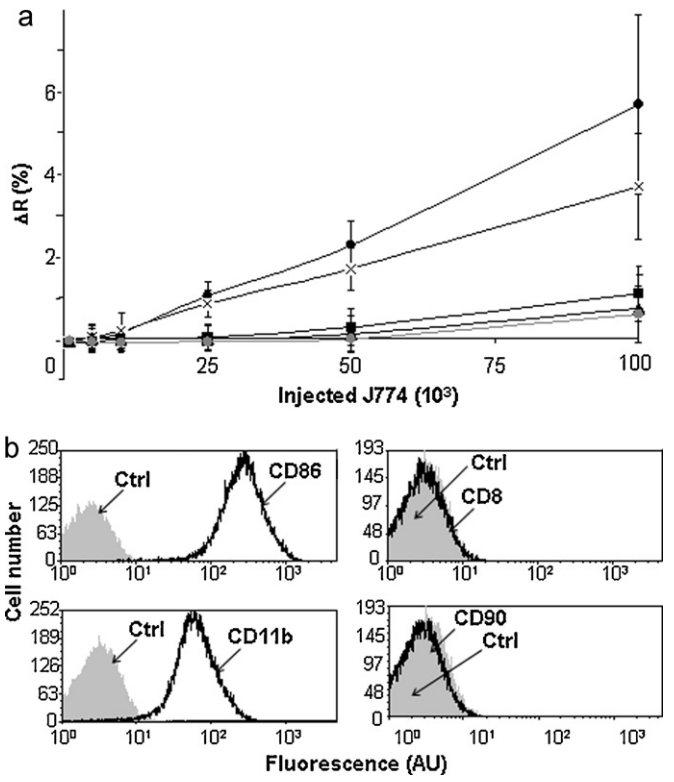

Fig. 2. SPRi signal correlation with the amount of injected cells in a mixed population. J774 were mixed with HL60 cells in different ratios, pre-incubated in the presence of 15% mouse serum and injected (2×10^5 total cells) onto a chip to which mAb (2 μM) were grafted. Cell binding was monitored by SPRi. (a) Signal (ΔR) obtained for each spot after 40 min injection; (●) anti-CD86, (×) anti-CD11b, (■) anti-CD90, (▲) anti-CD8, and (●) IgG control. Error bars are the standard deviations from triplicate measurements. (b) Flow cytometry analysis of levels of cell marker expression.

the SPR apparatus showing that each white spot corresponded to a cell (Supplementary Fig. 1).

To determine the sensitivity of the method, samples containing different ratios of J774/HL60 cellular mixture (from 0% to 50%) were injected, total cell number being maintained to 200,000. All injections were carried out successively, without chip regeneration. Thus measurements after each injection corresponded to cumulated signal. The SPRi signal on both anti-CD86 and CD11b spots correlated with the number of J774 injected. In these conditions, we could detect a population corresponding to ~5% of the overall injected cells, i.e. 10,000 total J774 cells. Again, signals obtained on anti-CD86 spots were higher than that obtained on anti-CD11b spots, whatever the J774/HL60 ratio (Fig. 2a).

Thus, the SPRi signal obtained upon cell binding on the Ab microarray depends on both cell number and targeted cell marker. In this last case, it is worth to notice that the two receptors are not expressed at the same density by J774, CD86 being 6 times more abundant than CD11b as shown by flow cytometry analysis (Fig. 2b).

3.2. Morphology of bound cells

As SPR signal depends on events taking place at the chip surface (Homola et al., 1999), it could be influenced by the shape of the bound cell. Thus, we wondered if the cellular protein targeted by the antibody impacted on cell spreading. To answer this question, we analyzed using confocal microscopy the morphology of the cells specifically bound to the Ab grafted on the chip. Images were compared to those obtained for cells attached to a surface via ionic interactions on polylysine-coated glass. To distinguish shape alterations, cellular membranes were stained using cholera toxin. Cells immobilized on polylysine presented rounded shape (Fig. 3a), whereas those captured via Ab–Ag interaction displayed a more flattened morphology (Fig. 3b). A significant majority (>70%) of cells bound to anti-CD86 presented a spread out and irregular shape (Fig. 3c). The contact area between cells and the substrate increased on average from 5 μm (polylysine surface) to 11 μm and 23 μm when bound to anti-CD11b and anti-CD86 Ab spots, respectively. Thus interaction of the cells with grafted Ab acts on their morphology.

3.3. Cell viability during the experiment

It was important to verify that our system did not adversely affect cell viability. So, we collected cells not retained on the microarray at the exit of the SPRi device and controlled their viability using EB/AO staining. The majority of cells recovered (>98%) showed good viability (data not shown). We then wondered whether the cells bound to the biochip via Ab–Ag interactions were also live. After cell injection (2×10^4) and signal stabilization, the prism was removed from the apparatus and cells were observed through a microscope after EB/AO staining (Supplementary Fig. 1c). In this case, the number of bound cells was estimated at about 700 cells/mm^2, and very few of them fluoresced orange (dead cells) whereas the majority fluoresced green (living cells). Thus cell viability was not affected by capture on the biochip. Moreover, the majority of bound cells (more than 90%) remain alive even after

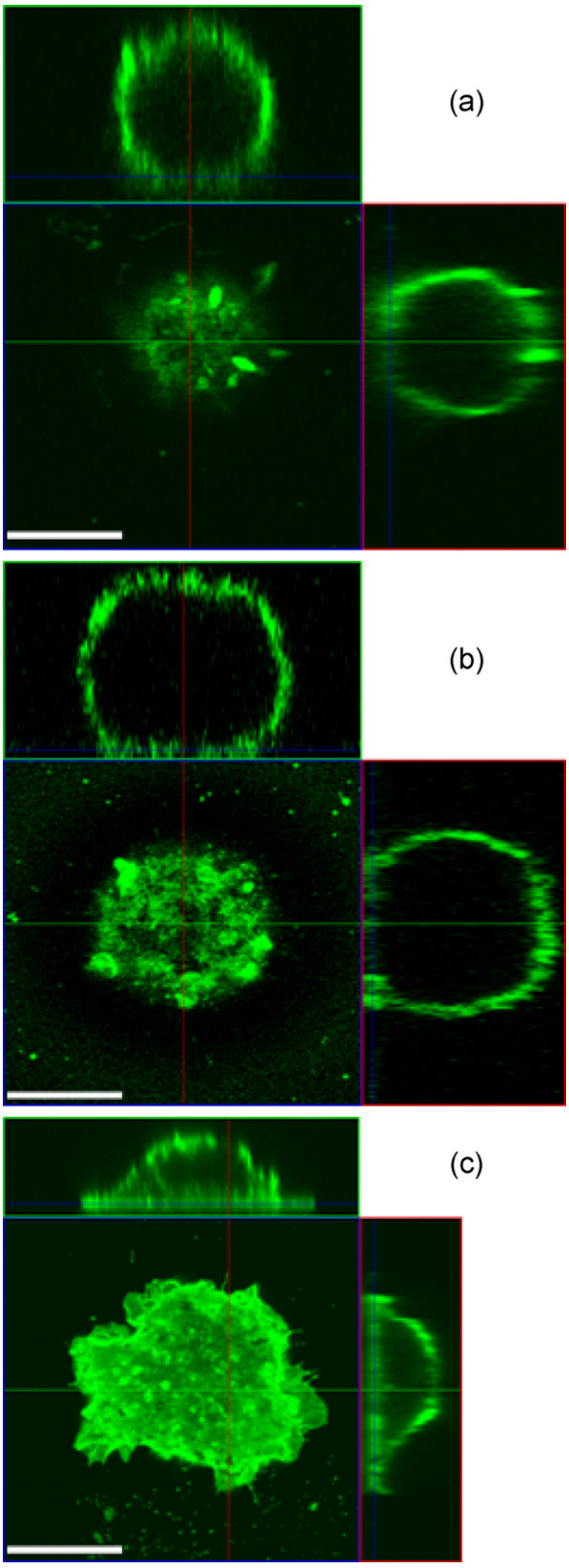

Fig. 3. Morphological analysis of cells bound to the chip by confocal microscopy. J774 cells (10^6 mL^{-1}) pre-incubated with 15% mouse serum were allowed to bind to a glass surface via non-specific (polylysine) or specific (Ab–Ag) interactions. Cell membranes were stained using fluorescently labeled cholera toxin B fragment. For each condition, we present a view of the cell–chip interface and two reconstructed images of orthogonal cross-sections (a) Polylysine-coated area. (b) Anti-CD11b area. (c) Anti-CD86 area. Scale bars: 10 μm.

24 h incubation on the biochip in a film of complete medium at 37 °C in a humidified 5% CO_2 incubator (data not shown).

3.4. Improvement of biochip efficiency

In spite of the good specificity of cell binding to spots, successive injections of a large cell numbers resulted in significant level of non-specific interaction between cells and the chip's gold surface, outside spots (Fig. 1b and 4a). To reduce non-specific binding, and at the same time enhance the sensitivity of cell detection, we developed biochips with a gold surface coated with PEO. PEO is known to have protein- and cell-repellent properties (Ruiz et al., 2008). The amphipathic properties of plasma-polymerized PEO make it bio-adhesive and anti-adhesive in dry and wet conditions, respectively, making it ideal for the creation of Ab microarrays and their subsequent use.

Microarrays were built on PEO-coated chips by direct microspotting of Ab onto the PEO surface. mAb remained stably adsorbed to the PEO-like film upon incubation in solution, while Ab-free regions were anti-adhesive in subsequent cell-based experiments.

Indeed, cell injection on such a chip led to a typical sensorgram (Supplementary Fig. 2). Successive injections of mixtures of J774 and HL60 cells at different J774/HL60 ratios were carried out as described above. Once again, we observed a specific, cell-concentration dependent signal. This signal reached plateau faster and was much stronger than that obtained on chips without PEO coating (Fig. 4b). Thus, analyses were more sensitive: a significant signal could be obtained for as few as 1000 bound cells. In our conditions, this corresponds to a cell population representing as little as 0.5% of the overall number of cells injected. In addition to improving sensitivity, PEO coating very efficiently prevented non-specific binding of cells to the chip's surface (Fig. 4a).

3.5. Analysis of cell receptor specificity

To assess the suitability of our system for studying the ability of cell receptors to bind their ligands, we analyzed macrophage trapping via their FcgR using grafted immunoglobulins. IgG from four different subclasses (IgG1, IgG2a, IgG2b and IgG3) were immobilized on PEO-coated chips. Injection of J774 (5×10^5) led to a significant signal on the different IgG spots, with a maximum for IgG2a (Fig. 5). This signal was partially or completely abolished when cells were preincubated with FcgR-blocking Ab, or with murine serum respectively, demonstrating that cell capture resulted from recognition of the grafted immunoglobulins by FcgR at the cell surface.

3.6. Analysis of complex biological samples

In addition to the analysis of cell lines, Ab microarray system could be useful to analyze primary cells isolated from donor or patient samples. To validate this application, we analyzed different cell populations derived from complex cellular samples such as blood. PBMC isolated from a healthy donor (28,000 cells) were injected onto a chip grafted with four different Ab specific for PBMC subpopulations: anti-CD3 (T lymphocytes), anti-CD14 (macrophages), anti-CD19 (B lymphocytes) and anti-CD56 (natural killer cells). To evaluate non-specific interactions, a negative isotypic control was also grafted. The highest signal was obtained for anti-CD3 spots, followed by anti-CD14 and anti-CD19. Finally, a small but specific signal was observed for the anti-CD56 spots. As shown in Fig. 6, these results correlate with the relative abundance of the different cell types in the PBMC population, as determined by flow cytometry: 62% CD3+, 14% CD14+, 2% CD19+ and 1% CD56+. Thus, in these conditions, our Ab microarrays are capable

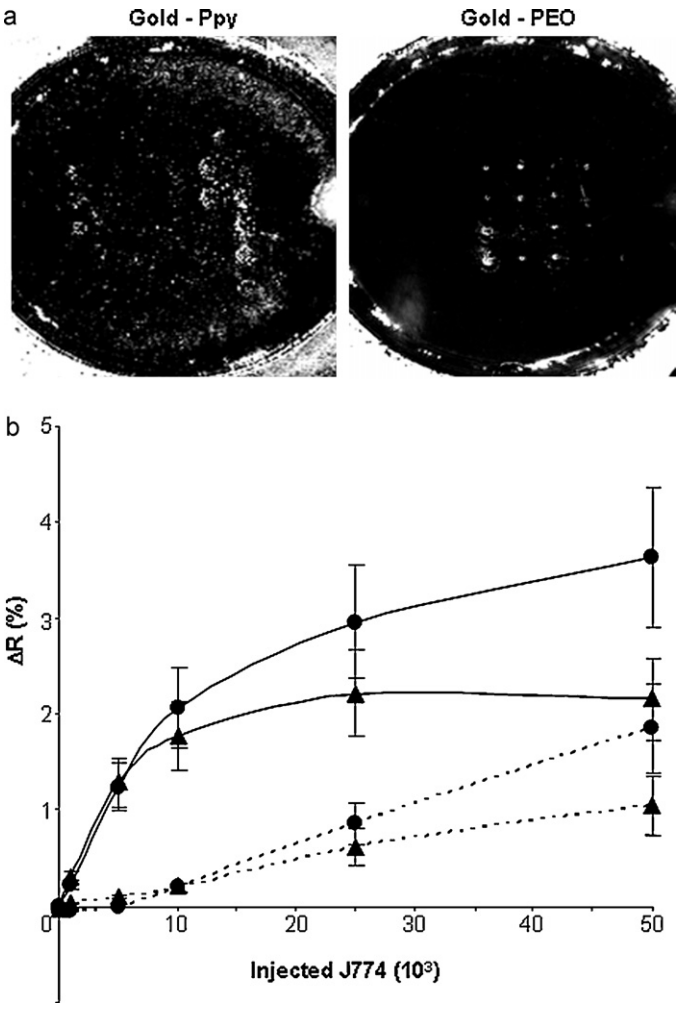

Fig. 4. PEO coating improves biochip efficiency. mAb (2 μM) were immobilized either on a gold surface via pyrrole electropolymerization, or adsorbed onto a gold surface coated with PEO. Mixed cell populations, containing both J774 and HL60 cells in different ratios (2×10^5 total cells) were pre-incubated with 15% mouse serum before injection. Cell binding was monitored by SPRi. (a) SPR differential images of the chip with or without a PEO film. (b) SPRi signal (ΔR) obtained for each spot on gold- (dotted lines) and PEO- (solid lines) coated chips; (●) anti-CD86, (▲) anti-CD11b. Values obtained on control spots (PEO without Ab) have been subtracted. Error bars are the standard deviations from triplicate measurements.

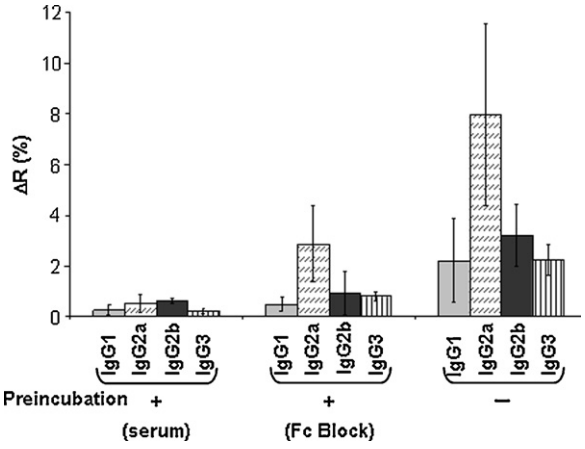

Fig. 5. Analysis of cell receptor specificity by SPRi. Different IgG subclasses (2 μM) were immobilized on a PEO-coated chip and J774 (2×10^5) cells were injected after pre-incubation in the absence or presence of mouse Fc block or mouse serum. Cell binding was monitored by SPRi. Signal (ΔR) obtained for each spot. Values obtained on control spots (PEO without Ab) have been subtracted. Error bars are the standard deviations from triplicate measurements.

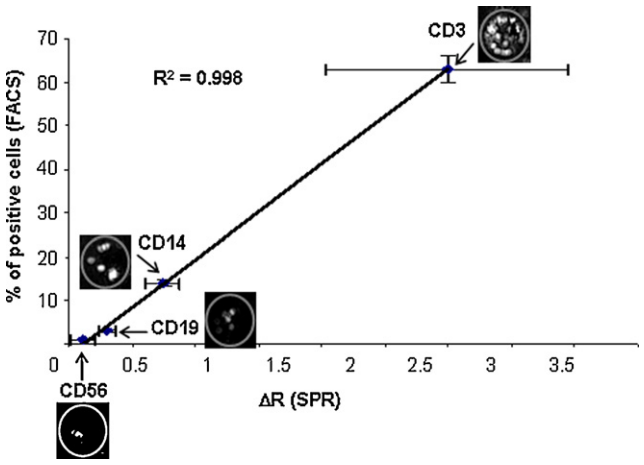

Fig. 6. Analysis of a human peripheral blood mononuclear cell population by SPRi. PBMC were pre-incubated in 15% human serum before injection (3×10^4) onto a PEO-coated chip grafted with different mAb (2 μM). Cell binding was monitored by SPRi and results were compared to those obtained by flow cytometry analysis of the same sample, using same mAb. ΔR and flow cytometry values correspond to the SPR signal and the percentage of positive cells respectively, obtained both for each mAb. The cell markers targeted by grafted mAb are indicated. A representative SPR differential image of each spot is provided. Values obtained on control spots (PEO with irrelevant Ab) have been subtracted. Error bars are the standard deviations from three measurements. R^2 = square of the correlation coefficient.

of quantitatively distinguishing different cell types within complex biological samples.

4. Discussion

The potential of SPR for biomolecular interaction analyses is great as it allows real-time measurement without the need for sample labeling. Moreover, SPRi enables simultaneous detection on several areas of the chip surface, making it suitable for parallel, high-throughput analyses (Liedberg et al., 1983; Rothenhäusler and Knoll, 1988). Combining Ab microarrays with SPRi is promising for rapid measurement of multiple parameters, as illustrated here in a system designed to analyze cells. Exposure of J774 cells to a gold surface on which various Ab directed against cell surface markers had been grafted, led to a strong, specific signal. In order for this technique to be adopted for "real" applications, it was necessary to demonstrate that it is harmless to the cells, as well as being sensitive and compatible with complex biological samples. Therefore, we checked cell viability after binding to the chip surface, and found almost all the cells to be alive, even after 24 h on the chip. Similar results were obtained after PEO coating (Supplementary Figs. 2 and 3). This is of great interest as it supports the use of the system not only for cell detection and quantification, but opens the possibility of downstream analyses of cellular responses.

Because SPR detection has a penetration depth of ~100 nm (Homola et al., 1999), the variation induced in the SPR signal by cell binding is not directly related to the whole cell (~10 μm diameter for J774 cells) but more closely to the part of the cell within a layer of about 100 nm above the chip's surface. Interestingly, whereas cells attached to the gold surface via non-specific interactions maintained their standard rounded shape, cells bound to Ab through surface proteins flattened out against the biochip. When this occurred, the part of the cell detectable by SPR increased, as the contact area was more important. In addition, we observed that the degree of cell flattening depended on the surface protein recognized by the Ab. Therefore, the SPR signal induced by cell binding depends, at least partly, on the target of the Ab grafted to the chip. It should be noted that we cannot exclude that cell spreading may be influenced by chip surface leading to a difference between gold–Ppy

and gold–PEO. Unfortunately, as PEO layer is unstable during the PFA treatment used to fix the cells before confocal analysis, we cannot verify this point.

Our results combining confocal microscopy and flow cytometry data, obtained using the same mAb clones as those used on our microarrays, suggest that cell flattening correlates with the cell surface density of the protein targeted by the Ab. Cell flattening is likely to be related to protein capping following receptor engagement by Ab. This mechanism, first described by Taylor et al. (1971), is a rapid sequence of events at the cell membrane. It is initiated immediately upon Ab binding and leads to redistribution, i.e. local concentration, of some surface molecules, in particular those targeted by the Ab. Movement of surface proteins is observed for instance when a cell interacts with Ab-functionalized beads (Canetta et al., 2005). In our case, this local concentration of surface molecules induces the formation of multiple interactions between the cell and the Ab grafted on the chip, involving a larger surface of the cellular membrane than in the case of non-specific binding. Thus, as the number of Ab-recognizing molecules present on the cell acts on cell flattening, it also influences the increase of reflectivity. These observations highlight the complexity of SPR signal, especially since other cellular events can be involved, such as changes in membrane composition or signal transduction (Yanase et al., 2010; Ziblat et al., 2006).

The cells used in this study (J774), expressed the costimulatory molecule CD86 at higher levels than the complement receptor CD11b (flow cytometry analysis Fig. 2b, Apolloni et al., 2000). Indeed, J774 cells bound to Ab microarrays yielded a higher signal for anti-CD86 spots than for anti-CD11b spots. Although we can not exclude an effect of Ab affinities, the difference in the SPRi signal obtained on anti-CD86 and anti-CD11b spots is likely due to the differing densities of these two molecules which modify the morphology of the bound cell, inducing a change in the mass gradient on the gold surface.

SPRi signal intensity is also related to the number of cells bound to spots. This follows a linear correlation, making our system suitable for the quantification of a given cell type, even in the presence of background cells. Here, we demonstrate the capacity of our initial system to detect a population representing 5% of the overall injected cells (i.e. 10,000 cells), with at least one order of magnitude of dynamic range. Following these observations, we attempted to improve this detection threshold, with a view to extending our system to the detection of tiny cell populations. For this, we modified the biochip's gold surface using PEO, a compound well known for its amphipathic properties, i.e. bio-adhesive and repellent in dry and wet conditions respectively (Ceriotti et al., 2009). Results obtained using PEO-coated chips highlight the various advantages of this surface: first, whereas the dynamic range remained unchanged, sensitivity was improved 10-fold, lowering the detection threshold to 1000 cells, representing 0.5% of injected cells; this value is below the detection limit usually obtained with biosensors (>2%) and in the order of those reported for the most efficient fluorescence-imaging based systems (<1%, Chen et al., 2005; Soen et al., 2003); second, the antifouling properties of PEO are such that, not only no saturation step is required, but successive cell injections do not lead to any of the non-specific cell binding that was problematic when using unmodified gold-surfaced chips. This is of importance since, unlike when the ligands used are proteins (Cherif et al., 2006), our attempts to regenerate chips after cell binding were unsuccessful. This is probably due to strong interactions between cells and Ab, because of antigen capping inducing multiple binding points, as discussed above. Finally, the bio-adhesive properties of PEO allow easy protein immobilization without any requirement for modification of the molecule.

Ligand–receptor interactions are key events in biology but their analysis requires labeling and is often based on indirect assays, using competition for instance (Féau et al., 2009). The system we describe here is suitable for this type of analysis and overcomes these limitations. Thus, J774 cells bind to different non-specific IgG immobilized on the chip. This binding is thought to involve cellular receptors, as these cells express three FcgR specific for different IgG subclasses: FcgRI (IgG2a), FcgRII (IgG1 and 2b) and FcgRIII (IgG3) (Weinshank et al., 1988). Indeed, IgG2a spots led to the highest signal as FcgRI is the most abundant FcgR on J774 cells (Heusser et al., 1977). Cell preincubation with murine serum, a source of IgG, leads to saturation of the FcgR, and abolished cell capture on the biochip. The specificity of IgG–FcgR interactions was confirmed by preincubating the cells with an anti-FcgR Ab known to specifically block their activity. In this case, cell binding was reduced (IgG2a) or suppressed (IgG1, 2b and 3). The reduced capacity of the Ab to block cell binding to IgG2a results primarily from its preferential binding to FcgRII and III, as indicated in the supplier's technical data sheet, secondarily from the high level of expression of FcgRI on J774 cells (Heusser et al., 1977).

One of the important challenges for the use of microarrays in the analysis of cell populations is their compatibility with complex biological samples. Until now, devices using SPR have been tested with samples containing only one or two cell types (Peelen et al., 2006; Suraniti et al., 2007; Yanase et al., 2007). SPRi has been also reported to be suitable for morphology analysis at single cell level (Yanase et al., 2010). In this article we demonstrate the compatibility of our system with the analysis of a highly complex cell population such as PBMC. 3×10^4 cells were enough to detect four cell types, including the natural killer cells which represent less than 5% of total peripheral blood mononuclear cells. As (i) the chosen targeted molecules are highly expressed at the surface of the different cell types and (ii) the corresponding IgG present good affinity, we can assumed that the different cells once bound to the grafted IgG present very similar morphologies. Thus, the SPR signal is related to the amount of cells present in the sample. Indeed, a very good correlation between SPRi signals and flow cytometry data was found, indicating the relevance, in these conditions, of the chip-based assay for cell quantification and evaluation of the distribution of cell populations in complex samples.

5. Conclusion

The combination of SPRi technology and Ab microarrays allows discriminative and quantitative cell detection together with high-throughput, label-free analysis of small number of cells in clinical samples in real-time. This approach offers promising perspectives for the analysis of complex cell populations, including the detection and identification of rare cells (blood cell populations, residual tumor cells for example). The fact that this technology appears not to affect cell viability makes downstream analysis of some of their functions possible (for instance receptor–ligand interactions, cell activation or death, etc.).

Acknowledgements

We thank Dr. T. Livache, Grenoble, for providing the peek flow cell chamber.

This work was partly supported by the Agence Nationale de la Recherche sur le Sida (ANRS).

Appendix A. Supplementary data

Supplementary data associated with this article can be found, in the online version, at doi:10.1016/j.bios.2011.04.016.

References

Apolloni, E., Bronte, V., Mazzoni, A., Serafini, P., Cabrelle, A., Segal, D.M., Young, H.A., Zanovello, P., 2000. J. Immunol. 165 (12), 6723–6730.

Bretagnol, F., Lejeune, M., Papadopoulou-Bouraoui, A., Hasiwa, M., Rauscher, H., Ceccone, G., Colpo, P., Rossi, F., 2006. Acta Biomater. 2 (2), 165–172.

Canetta, E., Duperray, A., Leyrat, A., Verdier, C., 2005. Biorheology 42 (5), 321–333.

Ceriotti, L., Buzanska, L., Rauscher, H., Mannelli, I., Sirghi, L., Gilliland, D., Hasiwa, M., Bretagnol, F., Zychowicz, M., Ruiz, A., Bremer, S., Coecke, S., Colpo, P., Rossi, F., 2009. Soft Matter 5, 1406–1416.

Chen, D.S., Soen, Y., Stuge, T.B., Lee, P.P., Weber, J.S., Brown, P.O., Davis, M.M., 2005. PLoS Med. 2 (10), e265.

Cherif, B., Roget, A., Villiers, C.L., Calemczuk, R., Leroy, V., Marche, P.N., Livache, T., Villiers, M.B., 2006. Clin. Chem. 52 (2), 255–262.

Dorries, R., 2001. Curr. Top. Microbiol. Immunol. 253, 219–245.

Féau, C., Arnold, L.A., Kosinski, A., Guy, R.K., 2009. J. Biomol. Screen. 14 (1), 43–48.

Grosjean, L., Cherif, B., Mercey, E., Roget, A., Levy, Y., Marche, P.N., Villiers, M.B., Livache, T., 2005. Anal. Biochem. 347 (2), 193–200.

Heusser, C.H., Anderson, C.L., Grey, H.M., 1977. J. Exp. Med. 145 (5), 1316–1327.

Homola, J., Yee, S.S., Gauglitz, G., 1999. Sens. Actuator B 54, 3–15.

Liedberg, B., Nylander, C., Lundström, I., 1983. Sens. Actuator 4, 299–304.

Parks, D.R., Bryan, V.M., Oi, V.T., Herzenberg, L.A., 1979. Proc. Natl. Acad. Sci. U.S.A. 76 (4), 1962–1966.

Peelen, D., Kodoyianni, V., Lee, J., Zheng, T., Shortreed, M.R., Smith, L.M., 2006. J. Proteome Res. 5 (7), 1580–1585.

Pernollet, M., Jouvin-Marche, E., Leroy, V., Vigan, I., Zarski, J.P., Marche, P.N., 2002. Clin. Exp. Immunol. 130 (3), 518–525.

Rothenhäusler, B., Knoll, W., 1988. Nature 332 (6165), 615–617.

Ruiz, A., Buzanska, L., Gilliland, D., Rauscher, H., Sirghi, L., Sobanski, T., Zychowicz, M., Ceriotti, L., Bretagnol, F., Coecke, S., Colpo, P., Rossi, F., 2008. Biomaterials 29 (36), 4766–4774.

Soen, Y., Chen, D.S., Kraft, D.L., Davis, M.M., Brown, P.O., 2003. PLoS Biol. 1 (3), E65.

Suraniti, E., Sollier, E., Calemczuk, R., Livache, T., Marche, P.N., Villiers, M.B., Roupioz, Y., 2007. Lab Chip 7 (9), 1206–1208.

Taylor, R.B., Duffus, W.P.H., Raff, M.C., de Petris, S., 1971. Nat. New Biol. 233, 225–229.

Thimme, R., Wieland, S., Steiger, C., Ghrayeb, J., Reimann, K.A., Purcell, R.H., Chisari, F.V., 2003. J. Virol. 77 (1), 68–76.

Villiers, C.L., Cretin, F., Lefebvre, N., Marche, P.N., Villiers, M.B., 2008. Mol. Immunol. 45 (13), 3509–3516.

Villiers, M.B., Cortes, S., Brakha, C., Lavergne, J.P., Marquette, C.A., Deny, P., Livache, T., Marche, P.N., 2010. Biosens. Bioelectron. 26 (4), 1554–1559.

Walker, L.J., Sewell, A.K., Klenerman, P., 2010. Clin. Exp. Immunol. 159 (3), 245–255.

Weinshank, R.L., Luster, A.D., Ravetch, J.V., 1988. J. Exp. Med. 167 (6), 1909–1925.

Wingren, C., Borrebaeck, C.A., 2006. OMICS: J. Integr. Biol. 10 (3), 411–427.

Yanase, Y., Hiragun, T., Kaneko, S., Gould, H.J., Greaves, M.W., Hide, M., 2010. Biosens. Bioelectron. 26 (2), 674–681.

Yanase, Y., Suzuki, H., Tsutsui, T., Hiragun, T., Kameyoshi, Y., Hide, M., 2007. Biosens. Bioelectron. 22 (6), 1081–1086.

Ziblat, R., Lirtsman, V., Davidov, D., Aroeti, B., 2006. Biophys. J. 90 (7), 2592–2599.